ELSEVIER

Polymer 42 (2001) 3883–3891

polymer

www.elsevier.nl/locate/polymer

Effects of low-molecular-weight additives on interfacial tension of polymer blends: experiments for poly(dimethylsiloxane)/poly(tetramethyldisiloxanylethylene) + oligo(dimethylsiloxane), and comparison with mean-field calculations

Y. Sakane[a], K. Inomata[a], H. Morita[b], T. Kawakatsu[c], M. Doi[c], T. Nose[a,*]

[a]*Department of Polymer Chemistry, Tokyo Institute of Technology, 2-12-1 O-okayama, Meguro-ku, Tokyo 152-8552, Japan*
[b]*Japan Chemical Innovation Institute, Research & Education Center, Nagoya University, Furo-Cho, Chikusa-ku, Nagoya 464-8601, Japan*
[c]*Department of Computational Science and Engineering, Nagoya University, Furo-Cho, Chikusa-ku, Nagoya 464-8601, Japan*

Received 9 March 2000; received in revised form 7 August 2000; accepted 9 September 2000

Abstract

The effects of low-molecular-weight additives on the interfacial behavior of polymer blends have been studied experimentally and theoretically. The measured interfacial tension near the critical solution temperature T_c for poly(dimethylsiloxane)/poly(tetramethyldisiloxanylethylene) as a function of temperature is merely shifted by the addition of oligo(dimethylsiloxane) corresponding to the decrease of T_c, giving only a subtle adsorption effect in interfacial behavior. Theoretical calculations have also been carried out for polymer/polymer/additive ternary systems using the square-gradient theory (SGT) and the dynamic mean-field (DMF) calculation. The experimental results are quite consistent with theoretical predictions. Further theoretical calculations demonstrate that higher molecular weights and less miscibility with matrix polymers are most effective for a large adsorption of additives in the interface, leading to a large reduction of interfacial tension. SGT and DMF are found to predict almost the same interfacial tension and composition profiles in ternary polymeric systems.

Keywords: Polymer blend; Interfacial tension; Additive

1. Introduction

The effects of added diluents on the interfacial tension of a polymer/polymer interface may be more than the simple diluent effect, owing to the adsorption of the diluent molecules at the interface. There must be the adsorption because the number of unfavorable contacts between the polymer segments of different components at the interface is reduced by the adsorption, which also leads to the relaxation of conformational restriction of polymer chains at the interface. On the other hand, the entropy force tends to make the distribution of diluent molecules uniform in the system. Therefore, it is a basic question in polymer interfaces, i.e. how much the diluent actually reduces the interfacial tension by adsorption of the diluent as well as the ordinary dilution effect. Leibler [1] theoretically investigated this problem for weakly phase separated polymer mixtures with a copolymer additive, and concluded that even in the case of block-copolymer additives a dominant effect of additives is the reduction of interfacial tension due to the shift of critical temperature by dilution. On the other hand, Hong and Noolandii [2] extensively studied the interfacial tension for polymer/polymer/solvent systems with a wide range of composition by using the self-consistent field calculation, and found that even in strongly segregated polymer blends, the adsorption of solvent is not expected to be appreciable. For its fundamental interest in polymer interfaces, a very few studies have been done to observe the effects experimentally, and compare theoretical predictions [3,4]. In this paper, we present experimental data for the interfacial tension of polymer blends with oligomers as additive near the critical temperature. We also make theoretical calculations by two types of approaches to compare with the experiments and make some further theoretical considerations for the adsorption effects and applicability of the theoretical treatments. The approaches are the square-gradient theory and the dynamic mean-field calculation.

* Corresponding author. Tel.: +81-3-5734-2132; fax: +81-3-5734-2888.
E-mail address: tnose@polymer.titech.ac.jp (T. Nose).

0032-3861/01/$ - see front matter
PII: S0032-3861(00)00706-0

Table 1
Characteristics of the polymer samples (all values are determined by size-exclusion chromatography with PDMS-standard)

Samples	M_w	M_w/M_n
PDMS	10,600	1.15
PTMDSE	17,000	1.12
ODMS	460	1.0

2. Experimental section

2.1. Materials

Poly(dimethylsiloxane) (PDMS) and poly(1,1,3,3-tetramethyldisiloxanylethylene) (PTMDSE) were prepared by the anionic polymerization of tri(dimethylsiloxane) and 1,1,3,3-tetramethyldisiloxanylethylene, respectively. The PDMS and PTMDSE polymerized were purified and fractionated by molecular weight. Oligo(dimethylsiloxane) (ODMS), used as a diluent, was a product of Shin-etsu Co. Ltd., which was substantially the pentamer of dimethylsiloxane. The characteristics of these materials are listed in Table 1.

2.2. Coexistence curve measurements

The compositions of the coexisting phases were measured by a specially designed refractometer. A blended sample was put in a square optical cell sealed at the top with a Teflon sheet fixed by a screw. The cell was dipped in reference liquid in a glass cell in such a way that the cell was tilted by 45° to the light beam with some thickness. Parts of the light running through different surfaces of the square cell were refracted differently at the surfaces. The difference in the directions of the refracted light transmitted through the sample can determine the compositions of the upper and lower coexisting phases of the phase-separated sample. Temperature could be increased up to more than 200°C, being controlled to within ±0.05°C. Mixtures of PDMS and poly(phenylmethylsiloxane) were used as reference. The details of the refractometer is described elsewhere [5]. The relation between the weight composition and the difference of refracted-light direction was calibrated before the measurements were taken. To obtain the composition in volume fraction, the following equations of density, ρ, as function of temperature t in °C, were used, which were obtained by density measurements using picnometers:

$\rho/(\mathrm{g/ml}) = 0.98788 - 9.363 \times 10^{-4}$ (t/°C) for PDMS;
$\rho/(\mathrm{g/ml}) = 0.92434 - 7.3987 \times 10^{-4}$ (t/°C) for PTMDSE;
$\rho/(\mathrm{g/ml}) = 0.9009(1 + 1.28 \times 10^{-3}$ (t/°C))$^{-1}$ for ODMS [6].

For ternary systems with additives, the quasi-binary approximation was used, i.e. it was assumed that the fraction of additives in the two phases were the same because of the small amount of additive.

2.3. Interfacial tension measurements

The interfacial tension of the phase-separated mixture was measured in the same way as in the previous study [5] using the sessile-drop method. The apparatus was a specially designed one. A drop of one of the coexisting phase with less density was formed on a Teflon plate hanging from the top in a sample glass cell. Its image was focused on the detector of a CCD camera, and size and profile were measured by image analysis. The blended sample was sealed in the glass cell and was first homogeneously mixed above the critical temperature. Then it was cooled down to the temperature of measurement. As the phase separation proceeded, the segregated PTMDSE-rich phase floated due to its lower density and accumulated on the hanging plate to form a drop in the PDMS-rich lower phase. The temperature was controlled to within ±0.05°C.

The value of $\gamma/g\Delta\rho$, with g and $\Delta\rho$ being the gravity constant and density difference between the coexisting phases, respectively, was evaluated from the size and profile of the drop by fitting of the drop profile computed by the Laplace equation. The interfacial tension γ was calculated from the values of $\gamma/g\Delta\rho$, with density difference $\Delta\rho$. The $\Delta\rho$ was evaluated from the measured coexistence curve described above. The details of the experiments and data analysis have been described elsewhere [6].

3. Square-gradient theory

The square-gradient theory (SGT) is adopted here to attempt to describe the interfacial tension of polymer mixtures. Although the theory is applicable to an interface with a very gradual change of composition at the interface only, it is known that the theory provides reasonably good approximations [7]. The system considered here is a ternary mixture of polymer 1, polymer 2 and a low-molecular-weight solvent or an oligomer. The present theoretical treatment is exactly the same as that previously presented for a ternary system of polymer/polymer/hole to describe the surface of polymer blends [8], but in this study the hole is replaced by a solvent or an oligomer. The details are described elsewhere [8]. The free energy of mixing, $\Delta_m f$, for the system is expressed in terms of their polymeric indices N_i, volume fractions ϕ_i and segment-interaction parameters χ_{ij} between components i and j as follows:

$$\Delta_m f = \frac{\phi_0}{N_0}\ln\phi_0 + \frac{\phi_1}{N_1}\ln\phi_1 + \frac{\phi_2}{N_2}\ln\phi_2 + \chi_{01}\phi_0\phi_1 + \chi_{02}\phi_0\phi_2 + \chi_{12}\phi_1\phi_2. \quad (1)$$

Here the free energy is per lattice volume υ, measured in units of k_BT with k_B and T being the Boltzmann constant and the absolute temperature, respectively, and the subscripts 0, 1, and 2 denote the solvent, polymer 1 and polymer 2, respectively. The compositions $\phi(e)$ of the coexisting phases at equilibrium are determined by equalities of

chemical potentials μ_i of the respective components. The chemical potentials can be derived from the free energy of Eq. (1) by a conventional way.

On the basis of the square-gradient theory [9], the interfacial tension γ is given by

$$\gamma = \frac{k_B T}{v} \int (\Delta f + f_{grad})\, dz \tag{2}$$

where the coordinate z is taken to be perpendicular to the interfacial plane, Δf is the local excess free energy due to the presence of the interface and f_{grad} is the excess free energy due to the presence of composition gradients $\dot{\phi}_i = d\phi_i/dz$ at the interface. Δf is given from Eq. (1) by using Eq. (3):

$$\Delta f = \Delta_m f - \sum_{i=0}^{2} \phi_i \Delta\mu_i(e) \tag{3}$$

where $\Delta\mu_i(e)$ is the chemical potential (of mixing) at the equilibrium phases. The gradient term f_{grad} is given by the sum of the following entropy and energy terms, i.e.

$$f_{grad} = f^s_{grad} + f^e_{grad} \tag{4}$$

with

$$f^s_{grad} = \frac{a_0^2}{\phi_0}\dot{\phi}_0^2 + \frac{a_1^2}{\phi_1}\dot{\phi}_1^2 + \frac{a_2^2}{\phi_2}\dot{\phi}_2^2, \tag{5}$$

$$f^e_{grad} = \frac{\chi_{01}\lambda_{01}^2}{2}\dot{\phi}_0\dot{\phi}_1 + \frac{\chi_{02}\lambda_{02}^2}{2}\dot{\phi}_0\dot{\phi}_2 + \frac{\chi_{12}\lambda_{12}^2}{2}\dot{\phi}_1\dot{\phi}_2 \tag{6}$$

where a_i is the statistical segment length, and λ_{ij} represents the range of distance within which the interaction between the i- and j-segments is working. Transforming the polymer fractions ϕ_i into the polymer composition $\theta = \theta_1 = \phi_1/(\phi_1 + \phi_2)$ with

$$\phi_1 = (1 - \phi_0)\theta; \qquad \phi_2 = (1 - \phi_0)(1 - \theta) \tag{7}$$

the interfacial tension is finally given by

$$\gamma = \frac{k_B T}{v} \int I\, dz \tag{8}$$

with

$$I \equiv \Delta f + g\dot{\phi}_0^2 + h\dot{\theta}^2 + k\dot{\phi}_0\dot{\theta} \tag{9}$$

where

$$g = \frac{1}{2}\{\chi_{01}\lambda_{01}^2\theta + \chi_{02}\lambda_{02}^2(1-\theta) - \chi_{12}\lambda_{12}^2\theta(1-\theta)\} + \frac{1}{36}\left\{\frac{a_0^2}{\phi_0} + \frac{a_1^2\theta + a_2^2(1-\theta)}{1-\phi_0}\right\}, \tag{10}$$

$$h = \frac{1}{2}\chi_{12}\lambda_{12}^2(1-\phi_0)^2 + \frac{1}{36}(1-\phi_0)\left(\frac{a_1^2}{\theta} + \frac{a_2^2}{1-\theta}\right), \tag{11}$$

$$k = \frac{1}{2}(1-\phi_0)\left[\{\chi_{02}\lambda_{02}^2 - \chi_{01}\lambda_{01}^2 + \chi_{12}\lambda_{12}^2(1-2\theta)\} - \frac{1}{18}(a_1^2 - a_2^2)\right]. \tag{12}$$

Minimizing the integration of Eq. (8) for γ, one can obtain the composition profiles at the interface and the value of γ at equilibrium. The equilibrium conditions yield

$$\frac{\partial I}{\partial \phi_0} - \frac{d}{dz}\left(\frac{\partial I}{\partial \dot{\phi}_0}\right) = 0, \tag{13}$$

$$\frac{\partial I}{\partial \theta} - \frac{d}{dz}\left(\frac{\partial I}{\partial \dot{\theta}}\right) = 0. \tag{14}$$

Also the following equation holds

$$\Delta f = g\dot{\phi}_0^2 + h\dot{\theta}^2 + k\dot{\phi}_0\dot{\theta}; \qquad I = 2\Delta f. \tag{15}$$

Therefore, one has

$$\gamma = \frac{2k_B T}{v} \int \Delta f\, dz. \tag{16}$$

Solving the simultaneous equations of either Eqs. (13) and (14) or Eq. (15) and one of Eqs. (13) and (14), one can determine θ and ϕ_0 as functions of z and evaluate γ by the integration of Eq. (16).

Numerical calculations can be carried out in the following procedures. The compositions of the equilibrium coexistence phases are first computed. Then, the simultaneous differential equations are solved with a given set of initial values of ϕ_0, θ, and their gradients at a starting position. In asymmetrical cases, the starting position is set far away from the center of the interface, while in the symmetrical case, it is set at the center of interface where $\theta = 0.5$. By trial and error with changing the initial value, one can obtain the stable solutions which give rational values of variables at bulk phases. The solutions of ϕ_0 and θ as a function of z correspond to the composition profile, giving the excess free energy Δf as a function of z to yield the interfacial tension by Eq. (16). The values of parameters required for the calculations are the polymeric indices N_i, the statistical segment length a_i, the interaction length scale λ_{ij}, and the interaction parameters χ_{ij}. The results of γ-calculations can be given by the reduced interfacial tension, γ^*_{SGT}, defined as

$$\gamma = \frac{k_B T a}{v}\gamma^*_{SGT} \tag{17}$$

where γ^*_{SGT} is a function of N_i, χ_{ij}, and λ/a with λ and a being, respectively, put as $\lambda = \lambda_{ij}$ and $a = a_i$ for any of i and j. Note that when $N_0 = 1$, then we put $a_0 = 0$.

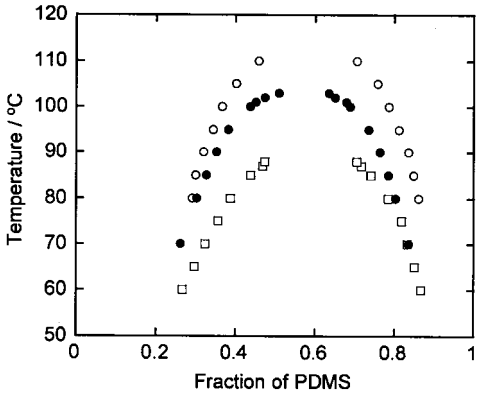

Fig. 1. Measured coexistence curve of the PDMS/PTMDSE blends with ODMSs of 0 wt.% (○), 3.2 wt.% (●), and 7.0 wt.% (□) as additives.

4. Dynamic mean-field calculation (self-consistent field theory)

Theoretical calculations based on the self-consistent field theory were performed by using the dynamic mean-field (DMF) calculation [10]. DMF, which is a dynamic version of the self-consistent field calculation, can be regarded as one of the many possible ways of iteration schemes that are used in obtaining the self-consistent field under the external conditions, such as the total incompressibility, total conservation of the segment density. It is guaranteed that the final equilibrium (or steady) state of the dynamic calculation corresponds to the equilibrium state of the static calculation. In the DMF simulation, the time evolution of concentration field $\{\phi_s(\boldsymbol{r})\}$ is pursued while calculating the free energy F of the system by using the path integral (Q_s) method. Here, s denotes the species of polymer chains (i.e. the components). The path integral is defined by the following diffusion equation:

$$\frac{\partial}{\partial i} Q_s(i,\boldsymbol{r}) = \left[\frac{a^2}{6}\nabla^2 - \frac{V_s(\boldsymbol{r})}{k_B T} \right] Q_s(i,\boldsymbol{r}) \tag{18}$$

with the initial condition

$$Q_s(0,\boldsymbol{r}) = 1 \tag{19}$$

where a is the segment length, and $V_s(\boldsymbol{r})$ the self-consistent field. The free energy F is expressed by [11]

$$\begin{aligned} F[\{\phi_s\},\{Q_s\}] = {} & -k_B T \sum_s M_s \ln\left[\int d\boldsymbol{r}_{N_s}\, Q_s(N_s,\boldsymbol{r}_{N_s}) \right] \\ & + W[\{\phi_s\}] \\ & - \sum_s \int d\boldsymbol{r} \left[\frac{\delta W}{\delta \phi_s(\boldsymbol{r})} \phi_s(\boldsymbol{r}) + V_s(\boldsymbol{r})\phi_s(\boldsymbol{r}) \right] \\ & - k_B T \sum_s M_s \ln M_s \end{aligned} \tag{20}$$

with

$$W\{\{\phi_s\}\} = \frac{k_B T}{\upsilon} \sum_s \sum_{s'} \int d\boldsymbol{r}\, \chi_{ss'} \phi_s(\boldsymbol{r}) \phi_{s'}(\boldsymbol{r}) \tag{21}$$

where M_s is the number of s-polymer chains. (N_s and $\chi_{ss'}$ are the same as those in SGT.) The time evolution of $\{\phi_s(\boldsymbol{r})\}$ is given by the following diffusion equation with the transport coefficient L:

$$\frac{d\phi_s(\boldsymbol{r},t)}{dt} = \nabla L \nabla \frac{\delta F}{\delta \phi_s(\boldsymbol{r})}. \tag{22}$$

The details of the DMF calculations have been described elsewhere [12]. Since we suppose a flat interface here, the system can be regarded as a one-dimensional system. In the case of a flat interface, the physical quantities are uniform in directions parallel to the interface, and change only in the perpendicular direction. Then, the three-dimensional path integral equation of Eq. (18), for instance, can be integrated with respect to the coordinates of parallel directions to give the one-dimensional version of Eq. (18). The calculations were carried out by using the one-dimensional versions of Eqs. (18)–(22). As the model adopted was for a canonical ensemble, the interfacial tension for macroscopic systems was calculated by the following basic equation for the definition of interfacial tension [13]:

$$\gamma = \frac{k_B T}{(\text{mesh-size})^2} \left\{ f - m \sum_{i=0}^{2} \mu_i(e) \right\} \tag{23}$$

where f is the free energy of the system with interface in units of $k_B T$, which is obtained by the present calculation, $\mu_i(e)$ is the chemical potential per segment in the bulk equilibrium phase in units of $k_B T$, which is calculated from the analytical equation of $\Delta\mu_i(e)$ [$\equiv \mu_i(e) - \mu_i^0(e)$] based on Eq. (1) with the chemical potential $\mu_i^0(e)$ of the pure component by DMF calculations, and m is the number of meshes. The number of meshes was set as 64 or 128. The mesh size corresponds to the segment length a. The value of L was chosen appropriately, so that the system reaches the final equilibrium state fast enough without numerical instability in the integration scheme. In the present study, we used $L =$ 5 or 10. The results for γ-calculations can be expressed in the reduced γ^*_{DMF} defined by

$$\gamma = \frac{k_B T}{a^2} \gamma^*_{DMF} \tag{24}$$

where γ^*_{DMF} is a function of N and χ. γ^*_{DMF} and γ^*_{SGT} are comparable with each other, which allows us to compare the results for the two theoretical treatments.

5. Results and discussion

5.1. Experimental results

5.1.1. Coexistence curves

Fig. 1 shows the measured coexistence curves for with

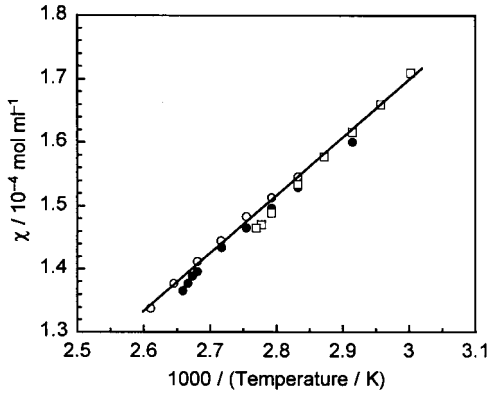

Fig. 2. Temperature dependence of segment-interaction parameters χ calculated from the measured coexistence curves by the Flory–Huggins theory for the PDMS/PTMDSE blends with ODMSs of 0 wt.% (○), 3.2 wt.% (●), and 7.0 wt.% (□).

and without the additive. The coexistence curve shifts to lower temperatures by increasing the amount of additive. From these results, the effective χ-parameter χ_{eff} for interactions between PDMS and PTMDSE were evaluated by the Flory–Huggins type free energy expression for the binary system so as to reproduce the composition difference between coexisting phases. Here, the polymeric indices were evaluated from the molar volumes, and χ values were given in the unit of mol/ml [5]. The results are shown as plots of $\chi_{\text{eff}}/(1-\phi_0)$ against temperature T in Fig. 2. The plots for different systems almost fall on a single curve except for those near the critical points. This indicates the validity of mean-field approximation because the effective χ_{eff} is given as $\chi_{\text{eff}} = (1-\phi_0)\chi$ under the quasi-binary assumption. The deviations near the critical points may come from a breakdown of the mean-field behavior due to critical fluctuations [5].

5.1.2. Interfacial tensions

Fig. 3 presents the temperature dependence of interfacial

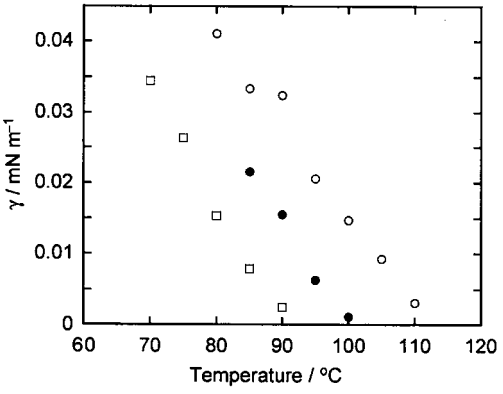

Fig. 3. Interfacial tensions for the PDMS/PTMDSE blends with ODMSs of 0 wt.% (○), 3.2 wt.% (●), and 7.0 wt.% (□) as additives.

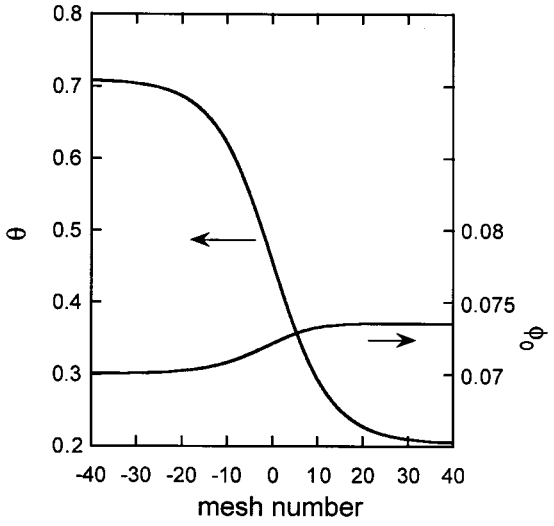

Fig. 4. Composition profiles at the liquid–liquid interface calculated by the square-gradient theory for the system of $N_0 = 6$, $N_1 = 191$, and $N_2 = 123$ with $\chi_{02} = 0$ at $\varepsilon = 0.1$. The composition of the 0-component in the component-1 rich phase is set to be 7%.

tension γ for different additive contents. The addition of oligomers makes the γ–T relation move to lower temperatures according to the shift of the critical solution temperature. This suggests that the adsorption effects of additive on γ are weak.

5.2. Results of square-gradient theory calculations

In the numerical calculations for the present experimental systems, we put $N_0 = 6, N_1 = 191$, and $N_2 = 123$ for ODMS, PTMDSE, and PDMS, respectively, and furthermore, we put $v = 96\ \text{ml mol}^{-1}$, $a_0 = a_1 = a_2 = 0.68\ \text{nm}$ and $\lambda_{01} = \lambda_{02} = \lambda_{12} = 0.5\ \text{nm}$ [6]. (In Refs. [5,6], N_0 for ODMS was set to be 5.57, while the round number, 6, was used here.) The value of front factor, $k_B Ta/v$, in γ^*_{SGT} (Eq. (17)) was approximated by $22\ \text{mN m}^{-1}$ at 100°C irrespective of temperature. The values of χ_{12} as a function of temperature were given by the relation obtained from the coexistence curve and were put as $\chi_{01} = \chi_{12} = \chi$ and $\chi_{02} = 0$.

The composition profiles at the interface at $\varepsilon = 0.1$ is shown in Fig. 4 as an example, where $\varepsilon = (\chi - \chi_c)/\chi_c$ with χ_c being χ at the critical point. Appreciable adsorption is not detectable. However, if one evaluates the excess amount of the additive at the interface by using the Gibbs dividing surface [13], one can see some positive excess additives, i.e. the adsorption is 0.0116 segments/segment-area in the system presented in Fig. 4 as an example, which must lead to an excess reduction of the interfacial tension by the adsorption although it may be very small.

The calculated interfacial tensions as a function of temperature and amount of additives are shown in Fig. 5. The calculated results reasonably reproduce the experimental ones in Fig. 3.

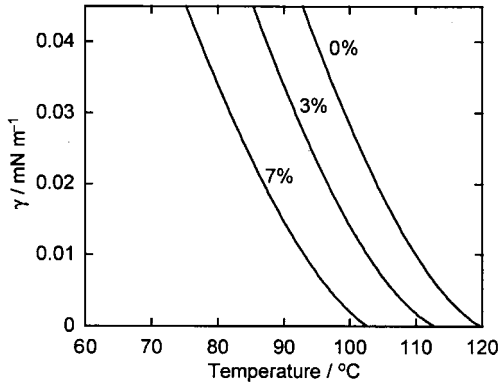

Fig. 5. Interfacial tensions calculated by the square-gradient theory for the system of $N_0 = 6$, $N_1 = 191$, and $N_2 = 123$ with $\chi_{02} = 0$ at different additive (0-component) contents indicated.

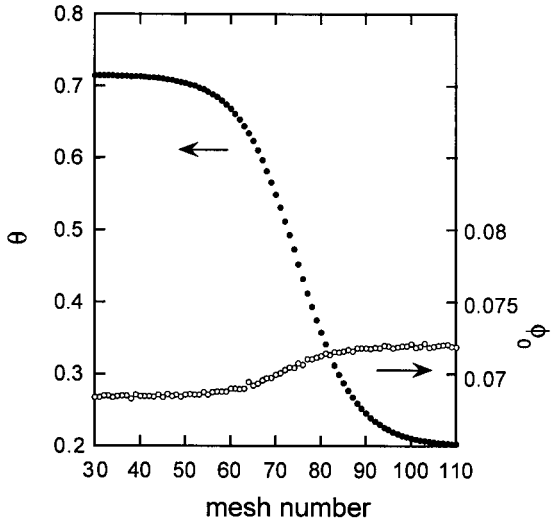

Fig. 6. Composition profiles at the liquid–liquid interface by the dynamic mean-field calculations for the system of $N_0 = 6$, $N_1 = 191$, and $N_2 = 123$ with $\chi_{02} = 0$ at $\varepsilon = 0.1$. The composition of the 0-component as a whole in the system is set to be 7%.

5.3. Results of dynamic mean-field calculations

Fig. 6 shows the composition profiles at the interface by the self-consistent field calculations for the case shown in Fig. 4 by the square-gradient method. The adsorption of additives defined by the Gibbs dividing surface is evaluated to be 0.0108 segments/segment-area for the case of Fig. 6, which is comparable with that (0.0116 segments/segment-area, shown above) obtained by the square-gradient calculation. It has to be noted here that, in the present DMF calculation, because of using the canonical ensemble, the bulk phase composition of additive, ODMS, is different from the set value of 7%, and not easy to be set at a desired value before calculation in general. The respective composition profiles calculated by the two treatments agree with each other quite well. The reduced interfacial tensions γ^* in this case are $\gamma^*_{SGT} = 0.00149(\lambda/a = 0.5/0.68 = 0.74)$ and $\gamma^*_{DMF} = 0.0016$ for SGT and DMF, respectively, showing a good agreement in γ between the two theoretical calculations. This implies that DMF predicts similar values of γ to those of SGT shown in Fig. 5, which are comparable to experimental values of γ presented in Fig. 3. Note that the results of SGT are not sensitive to the ratio of λ/a in general. For instance, $\gamma^*_{SGT}(\lambda/a = 1) = 0.00152$ for the above case, being very close to $\gamma^*_{SGT}(\lambda/a = 0.74)$.

5.4. General discussion

Theoretical calculations were carried out for the following general discussion by using both the approaches, SGT and DMF, where the value of λ/a is fixed to be unity in the calculations of SGT. The calculated results will demonstrate good agreements between these two treatments.

The present case is a weak segregation (near the critical) blend, where the adsorption effect is subtle, and the additive plays a role of diluent approximately only. If one can find a very good solvent to both components, i.e. a solvent having

Table 2
Interfacial tension and adsorption for polymer 1/polymer 2/additive systems($N_1 = N_2 = 30$; $\varepsilon = 0.2$) calculated by SGT and DMF

Systems	ϕ_{0b}[a]	χ_{01} ($=\chi_{02}$)	$10^3\gamma^*$		$(\phi_{0max} - \phi_{0b})/\phi_{0b}$		Γ	
			SGT	DMF	SGT	DMF	SGT	DMF
–	–	–	10.25	9.05	–	–	–	–
$N_0 = 1$	0.1	0	9.19	7.97	0.0101	0.0101	0.0061	0.0064
$N_0 = 5$	0.1	0	9.08	7.86	0.0481	0.0483	0.0400	0.0384
$N_0 = 30$	0.1	0	8.46	7.46	0.240	0.239	0.248	0.218
$N_0 = 100$	0.1	0	7.39	6.74	0.538	0.571	0.676	0.602
$N_0 = 100$	0.1	$\chi_{12}/4$[b]	6.59	6.52	0.762	0.840	1.085	0.915
$N_0 = 100$	[a]0.1	$3\chi_{12}/8$[b]	5.73	6.39	0.999	1.130	1.646	1.229
$N_0 = 30$	[b]0.01	0	10.05	8.76	0.300	0.292	0.0280	0.0256
$N_0 = 100$	[c]0.01	0	9.83	8.64	1.047	0.988	0.111	0.0896

[a] ϕ_{0b}: ϕ_0 in bulk phase. (In DMF calculations, ϕ_{0b} indicated in this column are the set value of ϕ_0, being slightly larger than real bulk compositions, which are [a]0.0966, [b]0.0096, and [c]0.0086 in respective cases.)

[b] $\chi_{12} = 0.08889$.

Table 3
Interfacial tension and adsorption for polymer 1/polymer 2/additive systems($N_1 = N_2 = 30$; $\varepsilon = 1.0$) calculated by SGT and DMF

Systems	ϕ_{0b}[a]	χ_{01} ($=\chi_{02}$)	$10^2\gamma^*$		$(\phi_{0max} - \phi_{0b})/\phi_{0b}$		Γ	
			SGT	DMF	SGT	DMF	SGT	DMF
–	–	–	6.75	5.86	–	–	–	–
$N_0 = 1$	0.1	0	6.04	5.23	0.0488	0.0491	0.0142	0.0192
$N_0 = 1$	0.1	$\chi_{12}/2$[b]	6.04	5.21	0.0494	0.0491	0.0173	0.0192
$N_0 = 1$	0.1	$3\chi_{12}/4$[b]	6.04	5.23	0.0497	0.0502	0.0179	0.0192

[a] ϕ_{0b}: ϕ_0 in bulk phase.
[b] $\chi_{12} = 0.14815$.

$\chi_{01} = \chi_{02} = 0$ or small interaction parameters, the additive would exhibit the adsorption effect. Another case where an appreciable adsorption effect may be expected is a strongly segregated blend. In reality, the theoretical calculations demonstrate that the goodness of interaction and the strong segregation are not enough to bring about the sufficient adsorption. In Tables 2 and 3 are shown numerical results of interfacial tension as the reduced one γ^* and the adsorption for the symmetrical blend of $N_1 = N_2 = 30$ at $\varepsilon = 0.2$ and 1.0, respectively. The adsorption is represented by the reduced maximum composition, $(\phi_{0max} - \phi_{0b})/\phi_{0b}$ with ϕ_{0b} being ϕ_0 in the bulk phase, of additives at the interface as well as the excess additive Γ. The composition profiles for $N_0 = 1$ with $\chi_{01} = \chi_{02} = 0$ are also shown in Fig. 7. Even very good solvents of $N_0 = 1$ do not adsorb much at the interface irrespective of segregation strength. It is noted that the adsorption Γ for $N_0 = 1$ is comparable to the present experimental case ($\Gamma = 0.0116$). The weak adsorption effect

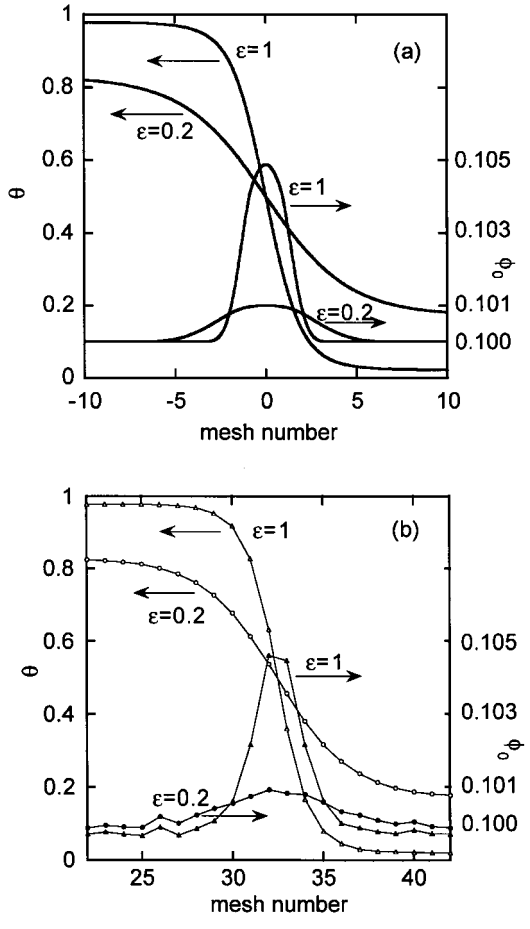

Fig. 7. Composition profiles at the liquid–liquid interface calculated by (a) the square-gradient theory and (b) the dynamic mean-field calculations for the system of $N_0 = 1$, $N_1 = 30$, and $N_2 = 30$ with $\chi_{01} = \chi_{02} = 0$ at $\varepsilon = 0.2$ and 1.0. The composition ϕ_0 of the 0-component as a whole in the system is set to be 10% in DMF, while ϕ_{0b} in the bulk phase is set to be 10% in SGT.

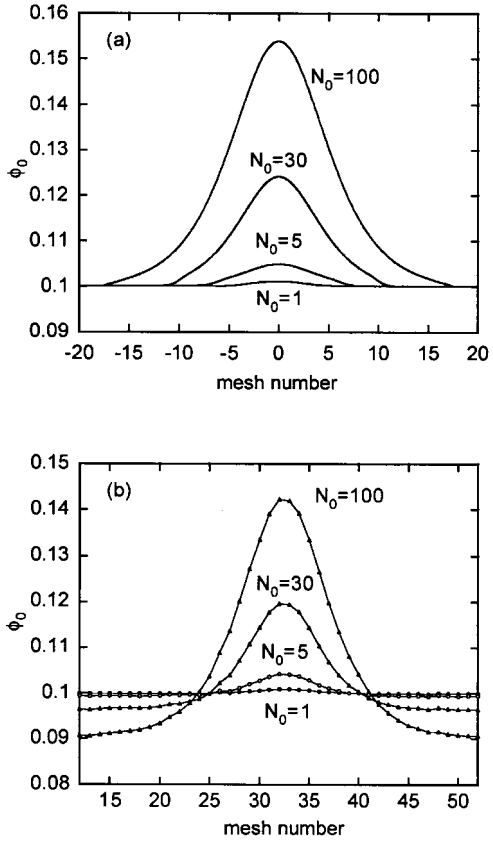

Fig. 8. Additive concentration profiles at the liquid–liquid interface calculated by (a) the square-gradient theory and (b) the dynamic mean-field calculations for the systems of $N_1 = 30$ and $N_2 = 30$ with different N_0s of additives having $\chi_{01} = \chi_{02} = 0$ at $\varepsilon = 0.2$ and around $\phi_{0b} = 0.1$.

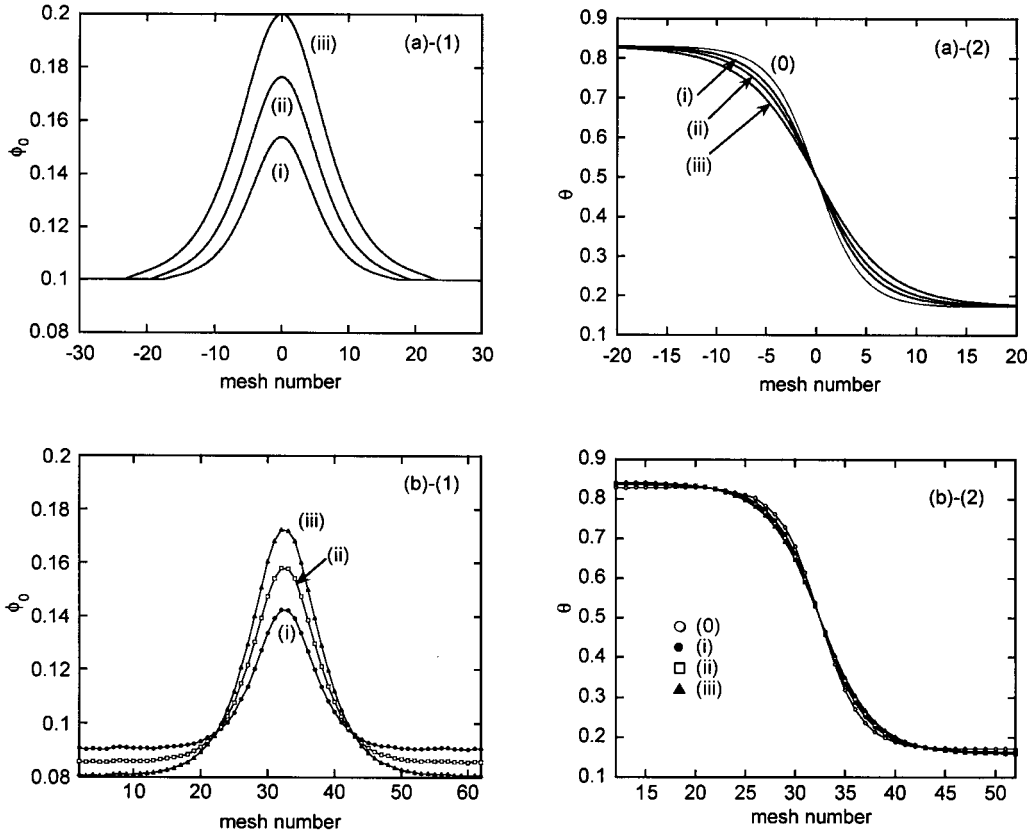

Fig. 9. Composition profiles at the liquid–liquid interface calculated by (a) the square-gradient theory and (b) the dynamic mean-field calculations for the systems of $N_1 = 30$ and $N_2 = 30$ with additives of $N_0 = 100$ having different values of $\chi_{01} = \chi_{02}$ at $\varepsilon = 0.2$ and around $\phi_{0b} = 0.1$. (1) Additive concentration profiles; (2) Matrix–polymer composition profiles; (i) $\chi_{01} = \chi_{02} = 0$; (ii) $\chi_{01} = \chi_{02} = \chi_{12}/4$; (iii) $\chi_{01} = \chi_{02} = 3\chi_{12}/8$; (0) no additives.

in the cases of $N_0 = 1$ may be due to the fact that the entropy effect of low-molecular-weight additives is strong enough to distribute additive molecules homogeneous in the system with the interface. Therefore, the molecular weight (or degree of polymerization) of the additive must be essential to have large adsorption and strong adsorption effect on the interfacial tension, which is shown in Fig. 8, which shows the molecular weight dependence of adsorption. In Table 2, the interfacial tension and adsorption for the corresponding systems are also shown. If the molecular weight of the additive is comparative with or more than those of the matrix blend, the adsorption becomes appreciable, and increases with increasing additive molecular weight, which leads to the reduction of interfacial tension with additives. The adsorption behavior is not essentially affected by the additive concentration, and the adsorption increases with increasing the amount of additives, but not as much as that expected from the proportionality, as seen in Table 2.

The effects of miscibility of additives to matrix blends are illustrated in Fig. 9 and numerically seen in Tables 2 and 3. As the additive become more immiscible to matrix polymers, i.e. as the χ-parameters χ_{01} and χ_{02} increase, the adsorption and the reduction of interfacial tension increase. This is quite understandable because the additives are less preferable (less comfortable) in the less miscible matrix and prefer to be at the interface.

In conclusion, larger adsorption effects are expected in higher molecular weight additives being barely miscible with both the matrix polymers. In general, however, one should notice that it is not easy, almost impossible to find such a polymer that is miscible to both component polymers of the matrix blend. The 50:50 random copolymer of A/B monomers, which may be treated as a homopolymer exhibiting $\chi_{01} = \chi_{02} = \chi_{12}/4$, may be an only candidate for a blend of A polymer and B polymer. See the case of $N_0 = 100$ with $\chi_{01} = \chi_{02} = \chi_{12}/4$ in Fig. 9 and Table 2.

Finally it is noted again that the square-gradient treatment (SGT) and the self-consistent mean-field calculation (DMF) give almost the same results in evaluations of interfacial tension and composition profiles for ternary polymeric systems. Also, it is pointed out again that SGT is not acceptable for the strong segregation in principle since it uses the Taylar expansion, although it usually gives rather reasonable results even for the strong segregation in numerical calculations. Furthermore we have to keep it in mind that the mean-field treatments, both of SGT and DMF, must break down near the critical point due to the critical concentration fluctuation, as has been mentioned for χ-parameter behavior evaluated

from the coexistence curve (Fig. 2). (See also Refs. [5,6] about the breakdown of mean-field treatment.)

6. Conclusions

The conclusions obtained in this study are as follows:

1. Addition of the oligomer ODMS to PDMS/PTMDSE merely shifts the χ–T relation corresponding to the decrease of the critical temperature, giving a subtle adsorption effect on interfacial behavior.
2. This is quite consistent with theoretical prediction. Theoretical calculations by SGT and DMF reproduce well the experimental results.
3. Higher molecular weights are the primary factor for a large adsorption on the interface.
4. Less miscibility of additives with matrix polymers is also effective for the large adsorption.
5. SGT and DMF predict almost the same interfacial behavior in ternary polymeric systems.

References

[1] Leibler L. Macromolecules 1982;15:1283.
[2] Hong KM, Noolandii J. Macromolecules 1981;14:736.
[3] Shinozaki K, Saito Y, Nose T. Polymer 1982;23:1937.
[4] Wagner M, Wolf BA. Macromolecules 1993;26:6498.
[5] Nose T. Polymer 1995;36:2243.
[6] Nose T. Macromolecules 1995;28:3702.
[7] Nose T. Polym J 1997;29:218.
[8] Nose T, Kasemura N. Polymer 1998;39:6137.
[9] Cahn JW, Hilliard JE. J Chem Phys 1958;28:258.
[10] Fraaije JGEM. J Chem Phys 1993;99:9202.
[11] Hong KM, Noolandi J. Macromolecules 1981;14:727.
[12] Hasegawa R, Doi M. Macromolecules 1997;30:3086.
[13] Defey R, Prigogine I, Bellemans A. Surface tension and adsorption. London: Longmans, 1966 (translated by Everett DH; chap. II).